

Full Length Research Paper

Raw, activated and modified biosorbents for the speciation of C. I. acid red 2 from aqueous solutions: An adsorption study

Richa Sharma¹, Soami P. Satsangee¹, Sudhir K. Verma^{1*}

Department of Chemistry, Faculty of Science, Dayalbagh Educational Institute, Agra, India.

Received 2 June, 2020; Accepted 7 October, 2020

Adsorptive removal of C. I. Acid Red 2 dye in the aqueous solution has been carried out on the various surfaces. This study describes the comparative adsorption of dye using mustard cakes (MC), sugarcane bagasse ash (SBA) and leaves of water hyacinth (WH) in different forms. The effects of initial adsorbate concentration, contact time, adsorbent dosage, temperature and pH of the medium on the adsorption of C. I. Acid Red 2 (C.I.A.R-2) or Methyl Red (MR) were investigated. The biosorbents were characterized by using modern technique (FTIR, SEM, and XRD). The maximum adsorption capacity of MR occurred at pH 2 and 4 for different adsorbent materials. Adsorption of the dyes was found to increase as the adsorbent dosage increases but decreases as initial concentration of the adsorbate (dye) increases. This is due to the fact that the active site of the adsorbent can adsorb a certain concentration of the dye. The C. I. Acid Red 2 adsorption kinetics was analyzed by using pseudo-first order and pseudo-second order kinetic models. The results indicated that the adsorption of C. I. Acid Red 2 (C-Colour, I-Index) onto various surfaces is best described using a pseudo-second order kinetic model. The Langmuir, Freundlich and Temkin adsorption isotherms were also studied and the data are well fitted with Freundlich isotherm. On the basis of the results it was demonstrated that mustard oil cake, sugarcane bagasse ash and leaves of water hyacinth are promising adsorbent materials which can be used to clean up textile dyes from wastewater.

Key words: C.I.A.R-2, sugarcane bagasse ash (SBA), mustard cakes (MC) and water hyacinth (WH), adsorption.

INTRODUCTION

The toxicity produced from the industrial wastes creates a major issue in environmental pollution and also in human health and their daily life. Due to the release of industrial wastes into the water bodies such as rivers and oceans has raised numerous problems associated with the health risk. Artificial dyes are widely used in industries for dyeing

and printing (Sandeep, 2010). The removal of colour from textile effluents has taken consideration over the last few years, not only of its toxicity but also due to its visibility. Traditional treatment facilities are often incapable to remove certain forms of colour, arising from reactive dyes as a result of their good solubility and low

*Corresponding author. E-mail: sudhirverma101@gmail.com.

biodegradability; thus, methods for decolourizing textile wastes are on the horizon (Vijayaraghavan et al., 2009). Over 10, 000 dyes production over 7×10^5 metric tonnes with an annual worldwide are available for industrial purposes and 5-10% of the dyestuff is improper in the industrial effluents. Therefore, there is a need to remove the color of dyes before the effluent is discharged into receiving water bodies. The most popular treatment methods for textile wastewater are combinations of biological treatment, chemical coagulation and activated carbon adsorption. Even discharging fewer amounts of dyes into water sources can affect the aquatic life and food web. Dyes can also create allergic dermatitis and skin problem. Some of the dyes have been reported to be oncogenic and mutagenic for marine organisms (Lorenc-Grabowska and Gryglewicz, 2007). The annual production of textile dyes is estimated to be over 80 Giga tonnes of which 10% are discharged as effluents (Zollinger, 1987). Releasing these dyes in water stream is aesthetically undesirable and has a serious environmental effect. Due to the colour, these decrease the sunlight penetration into the water. So, it affects aquatic plants (Jeremias et al., 2006). These can be categorized as follows (Yuzhu and Viraraghavan, 2002) anionic: direct, acid, and reactive dyes; cationic: basic dyes; and non-ionic: disperse dyes. Adsorption process has been proven as one of the best water treatment technologies around the world. Activated carbon is certainly considered as a universal adsorbent for the removal of diverse types of contaminants from water. However, given expansiveness and associated problems of regeneration, there is a constant finding for alternate inexpensive adsorbents. Several researchers have shown several inexpensive materials like clay (Tsai et al., 2005), narrow-leavedcattail (Inthorn et al., 2004), fly ash (Janos et al., 2003), wood dust (Garg et al., 2004) and alunite (Ozacar and Sengil, 2004), etc. The present work is focused on removing C. I. Acid Red 2 dye from their aqueous solution using adsorbents prepared from sugarcane bagasse ash, mustard oil cake, and leaves of water hyacinth.

Mustard cake (MC)

Mustard cake, about 60% of the seed, is generated as a by-product during extraction of the oil. India holds the third position in the world for the production of mustard cake is about 5.7 Mt every year (FAO, 1994). The composition of mustard cake varies with the variety, growing conditions and processing methods. The crude protein content varies from 33-40% of which 80-83% is true protein with an appreciable proportion of albumin, glutelin (Klockeman et al., 1997) and globulin. The protein is rich in lysine and Sulphur-containing amino acid which is limiting in cereal protein, making it excellent complementary to cereals in completing biological value of protein. Moreover, the composition of amino acids is

well balanced for application as a protein supplement for human nutrition.

Sugarcane bagasse ash (SBA)

Recently, several low costs, easily available and effective adsorbents were used for the removal of different dyes from aqueous solution. Many studies have been focused on the use of non-conventional low-cost adsorbents such as sugarcane bagasse, coconut husk, groundnut shell, banana pith, clay, rice husk (Prasetyko et al., 2006), maize cob, coir pith, orange peel and wheat straw dust in wastewater treatment. Instead of disposing of the sugarcane bagasse as a waste material, it has been used as an adsorbent for the removal of dyes from the wastewater. It mainly consists of cellulose (45%), hemicellulose (28%) and lignin (18%) and also it has carboxylic and hydroxyl groups, which are responsible for the uptake of dyes from wastewater (Ardejani et al., 2007; Hameed, 2009; Umesh et al., 2008).

Water Hyacinth (WH)

Water hyacinth (*Eichornia crassipes*) is an aquatic plant that lives and reproduces freely either on the surface of fresh waters or is anchored in mud. It grows in mats up to 2 m thick, thus reducing light and oxygen, and may change the aquatic chemistry, with significant negative effects on fauna and flora, causing an increase in water loss due to evaporate transpiration. It also causes problems for marine transportation, fishing, and at intakes for hydropower and irrigation schemes. This plant is now considered a serious threat to biodiversity (Hill et al., 1997), and, therefore, there is a strong desire to prevent its spread or eradicate its prolific growth.

In this investigation, the biomass from water hyacinth, an abundant, low-cost, and undesired plant material, was used for the purification of aqueous systems polluted with C. I. Acid Red 2. Herein, we report the adsorptive capacity of this biomass for dye elimination from aqueous systems, elaborating optimal conditions for the batch removal of C. I. Acid Red 2. Some surface properties of the biomass will also be covered.

MATERIALS AND METHODS

Preparation of adsorbents

Preparation of RMC, RSBA and RWH

The mustard cake was collected from local oil mill, sugarcane bagasse ash was collected from local sugar mill (The Kisan Sahkari Chini Mills" Ltd., Mahmudabad, Sitapur, Uttar Pradesh, India)) and water hyacinth was collected from Yamuna River at Dayalbagh, Agra, India. The collected mustard cake, sugarcane bagasse ash

and water hyacinth were washed with distilled water for several times to remove all the dirt particles. The washed materials are dried in oven at 80-110°C for 24 h. The dried biomasses were grounded to a fine powder by using mixer and sieved through 75 micron sieves. 25 g of sieved particles were repeatedly washed with hot distilled water. The sample was dried and stored (R-Raw, A-Activated and M- Modified).

Preparation of AMC, ASBA and AWH

The raw materials RMC, RSBA and RWH were dried overnight in an air oven. To prepare the activated mustard cake, sugarcane bagasse ash and water hyacinth refuse were treated with the solution of 20% of H₂O₂. The mixture was stirred with the help of magnetic stirrer at 60°C for 2 h and dried in an air oven at 80-100°C for 2 h. The heat-treated sample was washed several times with doubled distilled water until the filtrate is neutral (pH≈6.5-7.5) and its conductivity is minimal. These tests ensure that H₂O₂ and other ions which might be present are completely removed. The sample was dried, ground and sieved to uniform size of 75 micron.

Preparation of MMC, MSBA and MWH

This is one of the attractive ways of physical modification is to provide new desirable characters to chitosan and to synthesize chitosan and mustard cake, sugarcane bagasse ash and water hyacinth based bio composites by mixing or blending of chitosan and mustard cake, sugarcane bagasse ash and water hyacinth in the weight ratio of 1:1. In blending, at least two materials are mixed to obtain a new material with different physical properties. At thermodynamic equilibrium, the two materials of amorphous nature appear to be as a single-phase or homogeneous on blending with a new set of improved properties from the individual components. The miscibility and compatibility between the blended materials are decided by their mechanical and thermal properties. The method of blending is effective in practical application due to its simplicity in operation and availability of various organic compounds and natural polymers. Blending permits the wide range of properties by union of the components viz. chitosan and mustard cake, sugarcane bagasse ash and water hyacinth to achieve physically and chemically stable biopolymers required for the specific applications.

Adsorbate (C.I. Acid Red 2)

C. I. Acid Red 2 dye is a mostly used mono-azo dye in laboratory assays, textiles and other industrial products; however, it may cause serious issue in eye and skin (Chung et al., 1981) and pharyngeal or digestive tract irritation if inhaled or swallowed (So et al., 1990). Furthermore, C. I. Acid Red 2 is mutagenic under aerobic conditions: it undergoes biotransformation into 2-aminobenzoic acid and N, N-dimethyl-p-phenylene diamine (Wong et al., 1998; Vijaya and Sandhya 2003; Jadhav et al., 2008). It became imperative to develop low-cost adsorbent for the removal of C. I. Acid Red 2 dye from wastewater before being discharged into receiving water body.

The central objective of the work is to evaluate the adsorption performance of locally derived adsorbent from mustard oil cake, water hyacinth and okra seeds for the removal of MR dye from aqueous solutions. Adsorption equilibrium and kinetics were found. Isotherm equations were employed to quantify the adsorption equilibrium. The effects of solution pH, initial dye concentration and temperature on C. I. Acid Red 2 dye adsorption were also surveyed.

It has been suggested that the tough color of dyes could minimize turbidity (light penetration), and can affect the growth of benthic flora and fauna (Jadhav and Vanjara, 2004). Popular azo dye C. I. Acid Red 2(2-((E)-[4-(dimethyl amino) phenyl] diazenyl)

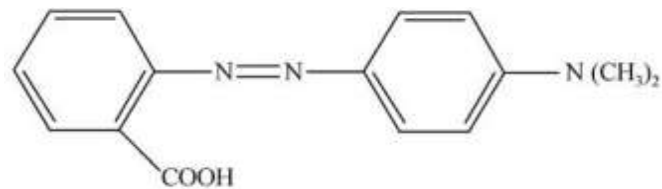


Figure 1. Molecular structure of the C. I. Acid Red 2.

benzoic acid; 1) was selected as a model system because the intense color (λ_{\max} 410 nm) in aqueous systems and also have low biodegradability due to the presence of benzene rings. The molecular structure of the C. I. Acid Red 2 is shown in Figure 1. The physico-chemical properties of C.I. Acid Red 2 are tabulated in Table 1 and the removal of C.I. Acid Red 2 onto various surfaces are shown in Table 2.

Preparation of (C.I. Acid Red 2) standard solution

C.I. Acid Red 2 (azo dye) supplied by local manufacturer was used for the study. 1×10^{-5} M stock solution was prepared by dissolving desired amount of it in 250 ml of distilled water and the required standard solutions were prepared by dilution method ($V_1M_1 = V_2M_2$). The prepared standard solution was used for bio-adsorption and for the study of adsorption isotherm.

EXPERIMENTAL PROCEDURES

Adsorption studies

Adsorption studies were performed by the batch technique. The adsorption of a C.I. Acid Red 2 on raw mustard cakes, raw sugarcane bagasse ash and raw water hyacinth activated mustard cakes, activated sugarcane bagasse ash and activated water hyacinth and modified mustard cakes, modified sugarcane bagasse ash and modified water hyacinth based biosorbents were obtained after stirring the beakers containing 50 ml of sample with different amount of adsorbents, different values of pH and different contact time at room temperature. The stirring proceeded for different periods after which the mixture was left to settle and filtered. The absorbance of the filtrate was determined by using UV-Vis spectrophotometer (Model DR 4000 U, HACH) at adjusted λ_{\max} (410 nm).

Equilibrium studies

A fixed amount of adsorbents (0.5 g) was added into a set of each 250 ml beakers containing 50 ml of different concentrations of C.I. Acid Red 2 solution with adjusted pH of 4.5. The beakers were stirred on a magnetic stirrer for 60 min until the equilibrium was reduced. The absorbance was measured by a double beam UV-Vis spectrophotometer (Model DR 4000 U, HACH). Each experiment was triplicated under identical conditions. The amount of adsorption at equilibrium, q_e (mg/g) was calculated by:

$$q_e = (C_0 - C_e) V/W \quad (1)$$

where, C_0 and C_e (mg/L) are the liquid-phase concentrations of dye at initial and at equilibrium time (t) respectively, V is the volume of the solution in liter (L) and W(g) is the mass of adsorbent used. The

Table 1. Physico-chemical properties of C.I. Acid Red 2. (Pub Chem).

S/N	Properties	Values
1	Molecular Weight	269.3 g/mol
2	Hydrogen Bond Donor Count	1
3	Hydrogen Bond Acceptor Count	5
4	Rotatable Bond Count	4
5	Exact Mass	269.116427 g/mol
6	Monoisotopic Mass	269.116427 g/mol
7	Formal Charge	0
8	Isotope Atom Count	0
9	Covalently-Bonded Unit Count	1

Table 2. Removal of C.I. Acid Red 2 onto various surfaces.

S/N	Adsorbents	pH	Temperature (°C)	Maximum % removal	Maximum adsorption capacity	References
1	Modified Zeolites	6.5	25	99	0.250 (g g ⁻¹)	Ioannou et al. (2012)
2	Activated carbon and multiwalled carbon nanotubes	1.0	30	96	14.08 (mg g ⁻¹)	Ghaedi et al. (2011)
3	Modified durian seed	6	30	92.52	401.65 (mg g ⁻¹)	Ahmad et al. (2015)
4	Tree bark powder	5	30	93.3	125.22 (mg g ⁻¹)	DIM (2013)
5	Iron Oxide nanoparticle	4	298-328 K	93	625(mg g ⁻¹)	Dadfarniaa et al. (2015)
6	Sugarcane bagasse	-	-	91	54.60 (mg g ⁻¹)	Azhar et al. (2005)
8	Modified banana trunk fibers	5	25 - 27	85	555.56 (mg g ⁻¹)	Rosemal et al. (2010)
9	EichorniaCrassipes biomass	8.0	30	99.7	8.85x10 ⁻² molg ⁻¹	Tarawou et al. (2007)
10	Banana Pseudostem fibers	2.08	27±2	98.98	93.515 (mg g ⁻¹)	Yet and Rahim (2014)
11	CNTs and activated carbon	-	-	95	200.0 mg g ⁻¹	Zare et al. (2015)
12	MWCNTs oxidized	-	-	97.5	108.7 (mg g ⁻¹)	Ghaedi and Kokhdan (2012)
13	AnnonaSquamosa seed	4.0	27±2	82.81	40.486 (mg g ⁻¹)	Santhi et al. (2010)
14	Pomelo peels	6.5	25	93.5-94.8	207.02 (mg g ⁻¹)	Tanzim and Abedin (2015)
15	Rice hulls	3	293 K	89	596.05 (mg g ⁻¹)	Hassan and Abdulhussein (2015)
16	Guargum powder	4.2	34	76	66.66 (mg g ⁻¹)	Saxena and Sharma (2016)
17	Sugarcane bagasse pith	5	30	86	75.55 (mg g ⁻¹)	Alaguprathana and Poonkothai. (2017)

percentage of dye-removal is calculated by following formula:

$$\text{Removal \%} = \frac{C_0 - C_t}{C_0} \times 100 \quad (2)$$

Where, C_t (mg/L) is the liquid-phase concentrations of dye at time (t).

Effect of contact time

The contact time ranged from 60 min, pH of the aqueous dye solution was adjusted to pH 4.5. The amount of adsorbent was 0.5g/50 ml. The dye concentration was 1×10^{-5} M.

Effect of pH

The pH ranges from 2.0 to 5.0; the amount of adsorbent was 0.5 g/50 ml, where the contact time was 60 min. The pH was adjusted by adding a few drops of 0.1 M NaOH or 0.1 M HCl.

Effect of amount of adsorbent

The range of amount of adsorbent was 0.5 g for 50 ml solution. The pH was fixed at 4.5 and the contact time for the experiment was 60 min.

RESULTS AND DISCUSSION

Characterization of new adsorbents

Fourier transform infrared spectroscopy (FT-IR)

The FT-IR spectrum of Pre and Post RMC, AMC, MMC, RSBA, ASBA, MSBA, RWH, AWH and MWH are illustrated in Figures 2 to 4. The functional groups assignment is summarized in Table 3a, b and c.

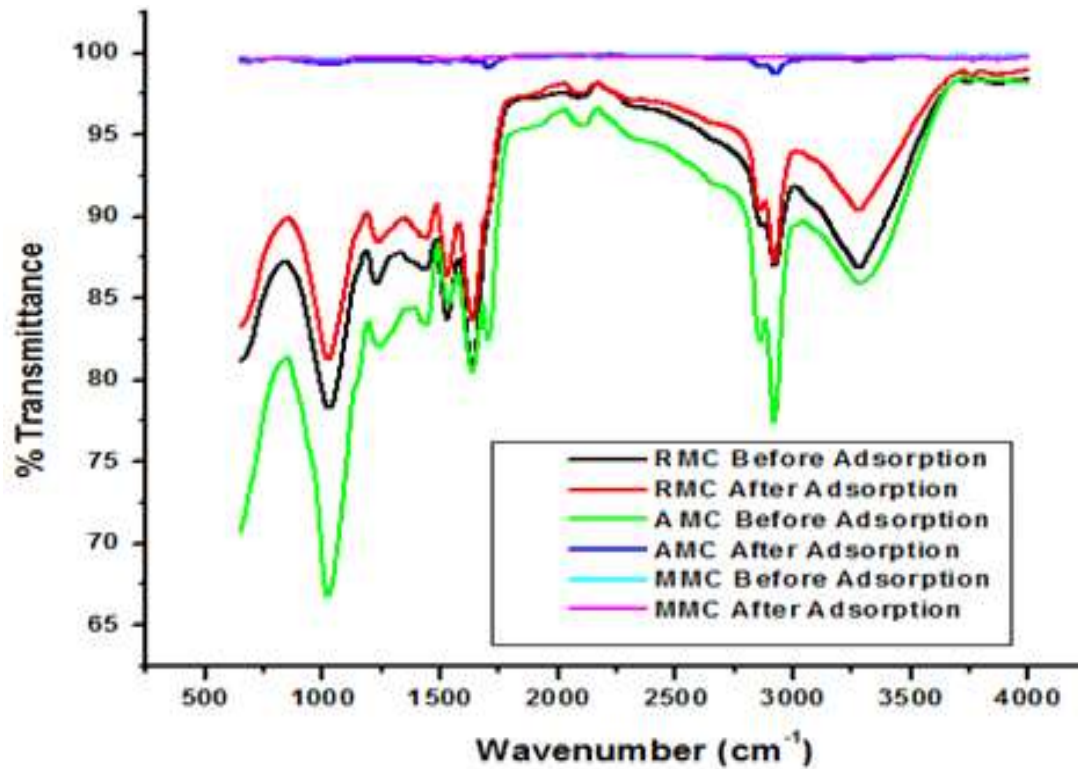


Figure 2. FTIR of Pre and Post RMC, AMC and MMC.

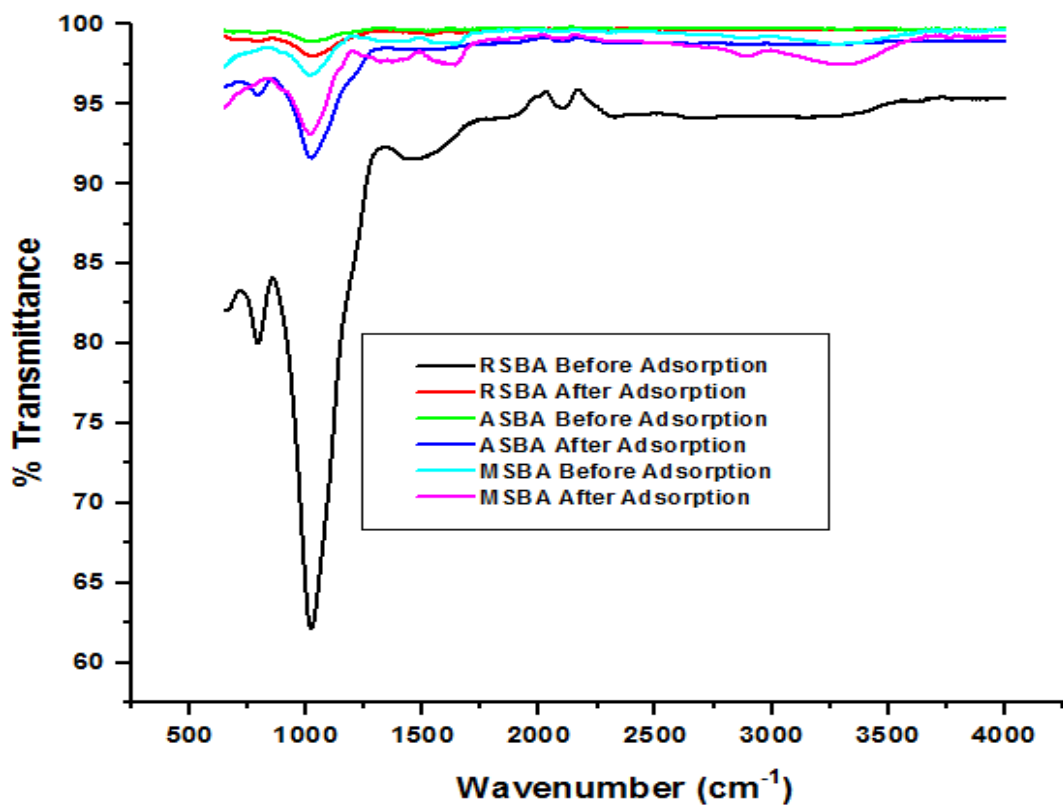


Figure 3. FTIR of Pre and Post RSBA, ASBA and MSBA.

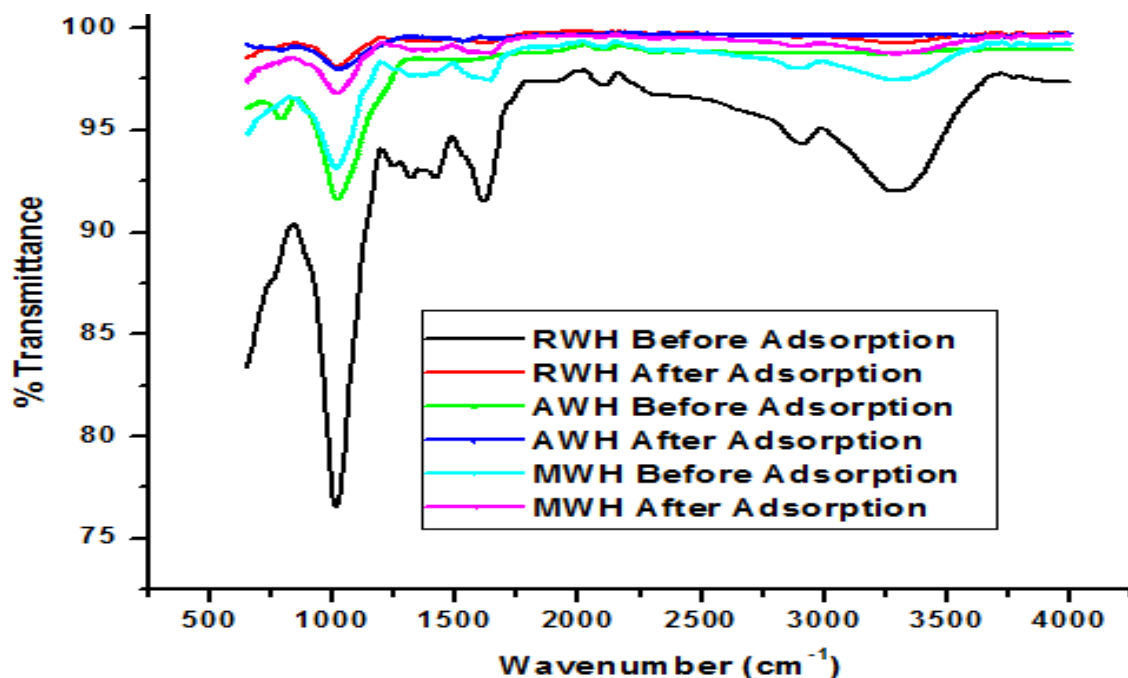


Figure 4. FTIR of Pre and Post RWH, AWH and MWH.

Table 3a. FTIR spectral characteristics of RMC, AMC and MMC before and after adsorption.

RMC			AMC			MMC			Peak assignments
*	**	***	*	**	***	*	**	***	
876	876	0	890	-	890	-	-	-	Si-OH band stretching
2344	2235	109	2344	-	2344	-	-	-	C≡H stretching
1468	1468	0	1468	1650	818	-	-	-	Aromatic C=C bond
1119	1119	0	1119	-	1119	-	-	-	C-OH stretching
1000	1000	0	1000	980	20	1054	-	1054	C-O stretching vibrations
1745	1745	0	1700	1750	50	-	-	-	OH deformation coupled
1231	1231	0	1231	-	1231	-	-	-	C-O stretching vibrations
3464	354	10	3472	3445	27	3723	-	3723	Surface hydroxyl groups
2927	2927	0	2927	3000	-73	-	-	-	Asymmetric C-H stretching

*Before Adsorption (cm^{-1}); **After Adsorption (cm^{-1}); ***Differences.

X-ray diffraction analysis

The XRD patterns of new biosorbents are illustrated in Figures 5 to 7. The broad diffraction peaks assignment is summarized in Table 4.

Scanning electron microscopy (SEM) analysis of new biosorbents

SEM micrographs of new biosorbents are presented in Figures 8 to 14. There are irregular pores distributed

which enhance the process of adsorption. The biosorbent surfaces resemble sponge like structure wherein ions may be trapped in the holes. The results show that there is uneven surface morphology with significant pores and fibrous structure

Adsorption results

Effect of contact time

50 ml of C.I. Acid Red 2 dye solution with known initial

Table 3b. FTIR spectral characteristics of RSBA, ASBA and MSBA before and after adsorption.

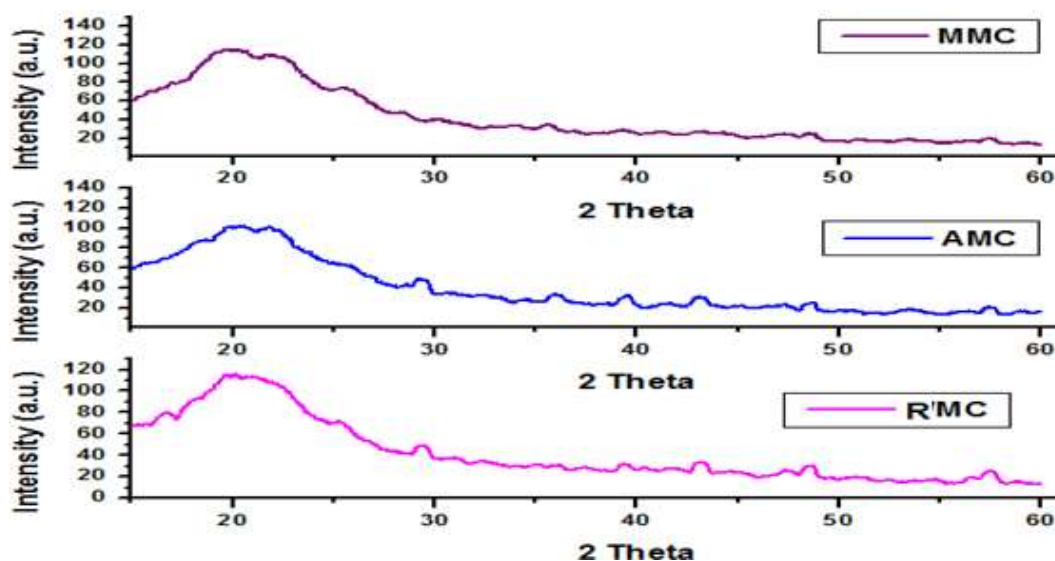
RSBA			ASBA			MSBA			Peak assignment
*	**	***	*	**	***	*	**	***	
1456	-	1456	1520	-	1520	1520	-	1520	Symmetric bending of CH ₃
2915	-	2915	2945	-	2945	-	2960	2960	Aliphatic CH group
1623	-	1623	1642	1650	8	-	1765	1765	C=O stretching
1087	1090	3	1100	1095	5	1100	1095	5	C-O stretching
1526	1530	4	1528	1545	-17	1526	1555	-29	Secondary amine group
791	791	0	1100	1100	0	1126	1150	-24	Si-O bending
-	-	-	-	-	-	-	3235	3235	Si-OH

*Before Adsorption (cm⁻¹), **After Adsorption (cm⁻¹), ***Differences.

Table 3c. FTIR spectral characteristics of RWH, AWH and MWH before and after adsorption.

RWH			AWH			MWH			Peak assignment
*	**	***	*	**	***	*	**	***	
3437	3437	0	-	-	-	3437	-	3437	Stretching vibrations of OH groups
2927	2927	0	-	-	-	2927	3000	-73	Asymmetric C-H Stretching
1000	1015	15	1000	1000	0	1000	1000	0	C-O-C stretching
765	765	0	725	725	0	780	755	25	Si-O-Si stretching
1050	1050	0	-	-	-	1050	1050	0	C-O-C stretching
1317	-	1317	-	-	-	-	-	-	Aromatic C-O and Phenolic OH
1416	-	1416	-	-	-	-	-	-	C-H
1636	1645	-9	-	1640	1640	1640	1640	0	Aromatic C-O-C-C

*Before Adsorption (cm⁻¹), **After Adsorption (cm⁻¹), ***Differences.

**Figure 5.** X-Ray Diffraction analysis of RMC, AMC and MMC biosorbents.

concentration was put in a series of 250 mL Erlenmeyer flasks. The amount of adsorbent that was added to each

flask was fixed at 0.5 g. The flasks were placed in an isothermal water bath shaker at constant temperature of

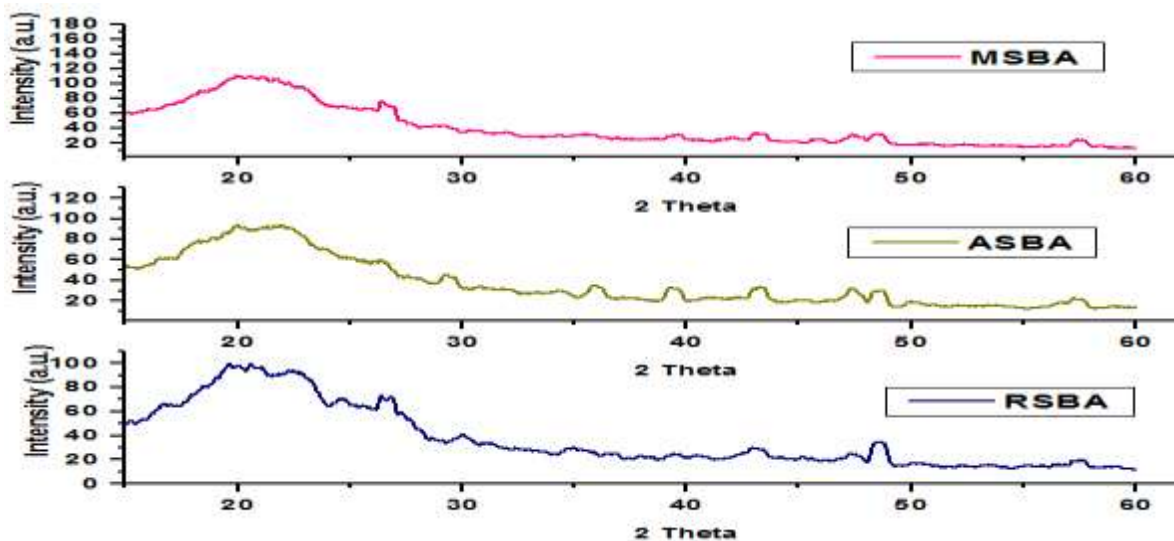


Figure 6. X-Ray Diffraction analysis of RSBA, ASBA and MSBAs.

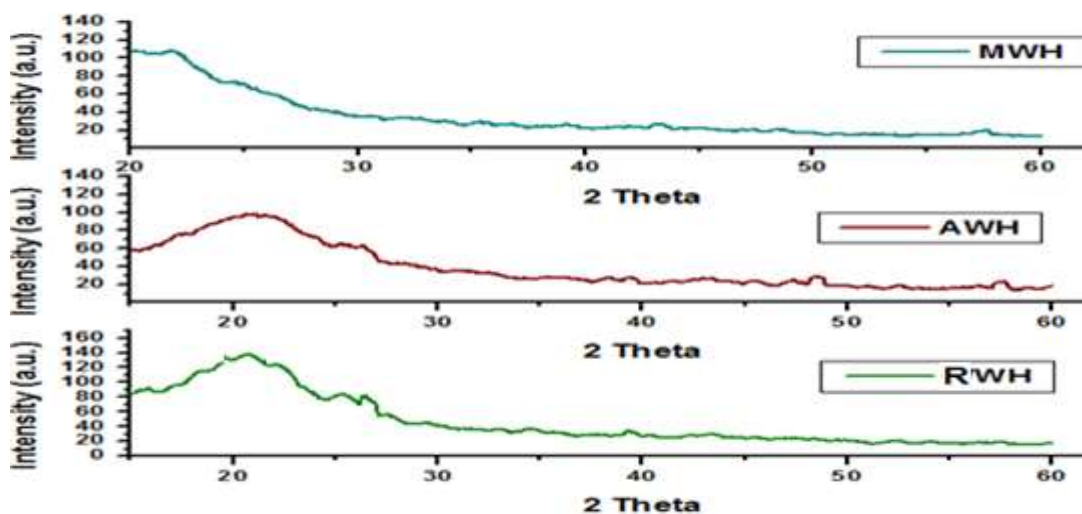


Figure 7. X-Ray Diffraction analysis of RWH, AWH and MWH biosorbents.

Table 4. XRD spectral characteristics of the adsorbent materials.

Value of $2\theta^0$	Plane	Crystallized fractions
40-50	101	Carbon
15-30	002	Carbon (C-H)
20	110	Semi crystalline chitosan
25	002	Graphite crystallite
49.5	002	Graphite crystallite

40°C, until equilibrium point was reached. Samples are withdrawn at intervals to determine the residual

concentration of the dye at 410 nm wavelength using an UV-Vis spectrophotometer (Model DR 4000 U, HACH).

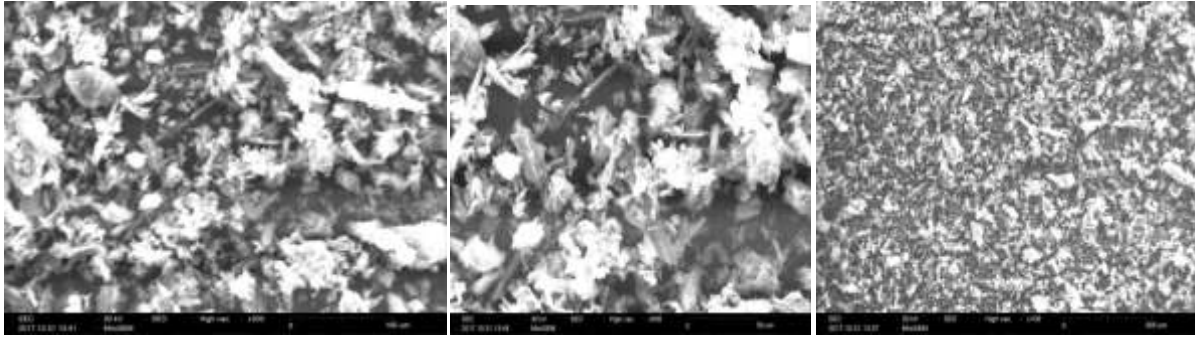


Figure 8. Scanning Electron Microscopy analysis of RMC, AMC and MMC biosorbents.

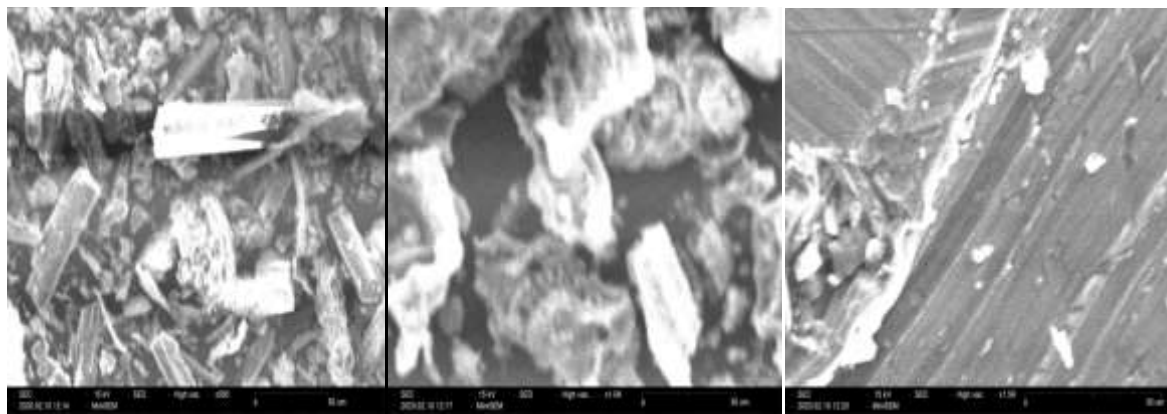


Figure 9. Scanning Electron Microscopy analysis of RSBA.

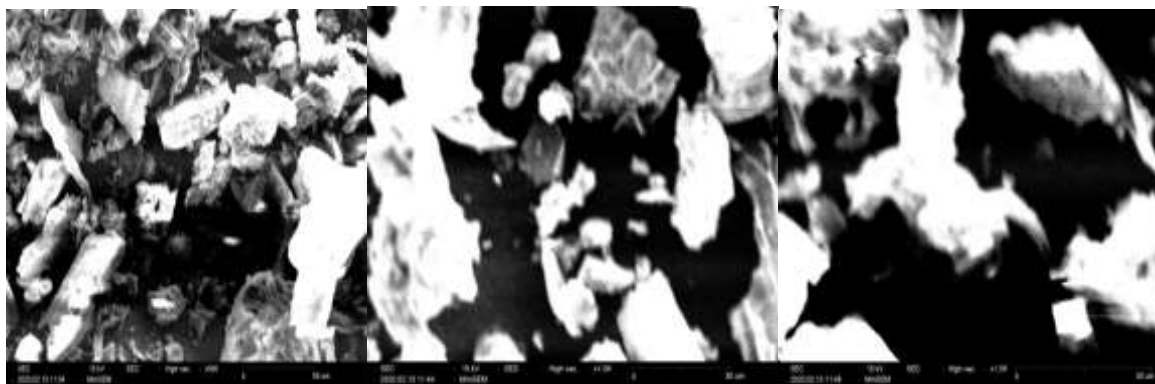


Figure 10. Scanning Electron Microscopy analysis of ASBA.

Figure 15 show the plot of contact time versus percentage of the dye removed C.I. Acid Red 2.

Effect of adsorbent dose

An increase in the adsorbent dose (RMC, AMC, MMC,

RSBA, ASBA, MSBA, RWH, AWH and MWH) from 0.1 to 0.6 g/50 ml increases the percentage of the dyes removed. This may be attributed to increased sorbents surface area and availability of more sorption sites resulting from increased dose of the sorbent. The increase in adsorbent dose at constant dye concentration and volume results to increased availability of sorption

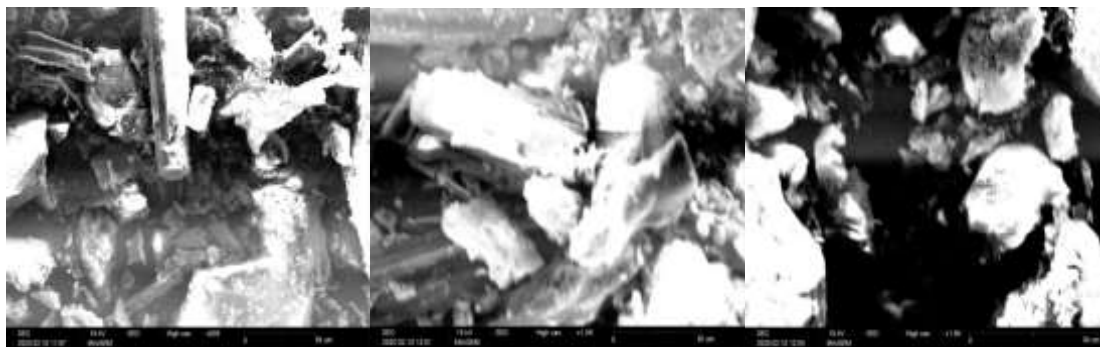


Figure 11. Scanning Electron Microscopy analysis of MSBA.

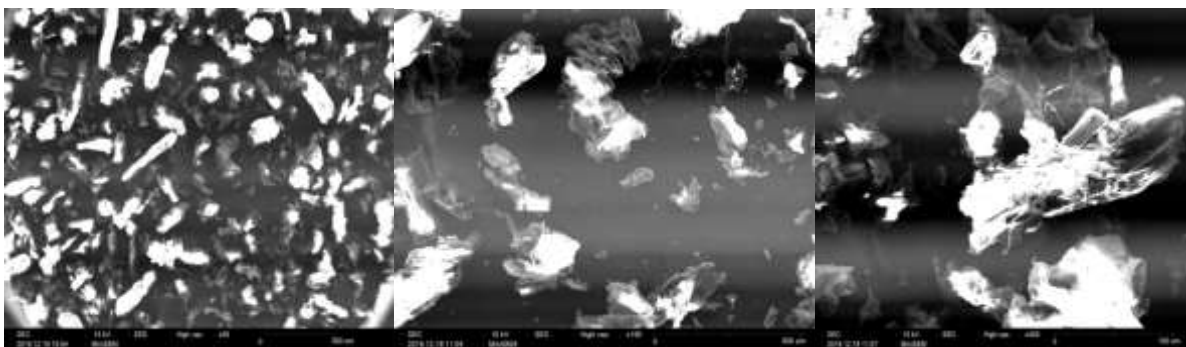


Figure 12. Scanning Electron Microscopy analysis of RWH.

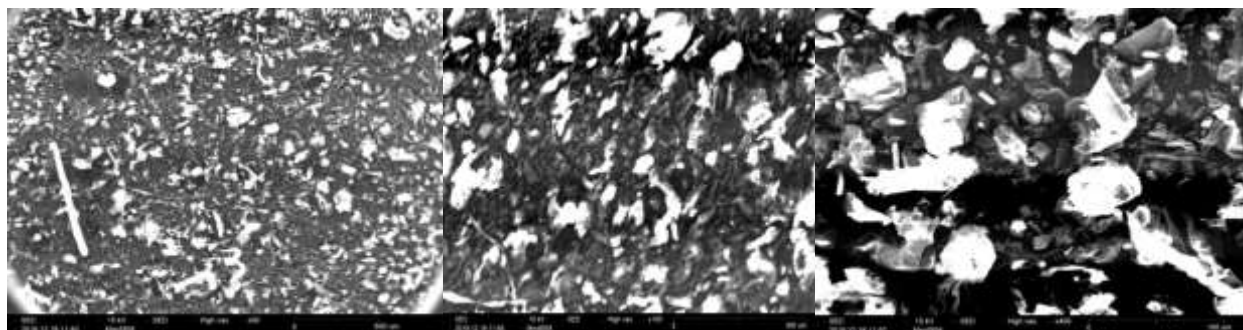


Figure 13. Scanning Electron Microscopy analysis of AWH.

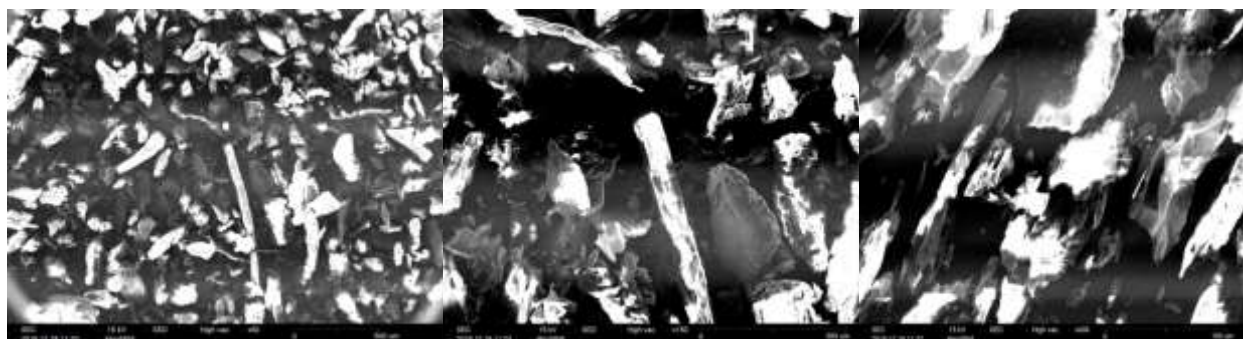


Figure 14. Scanning Electron Microscopy analysis of MWH.

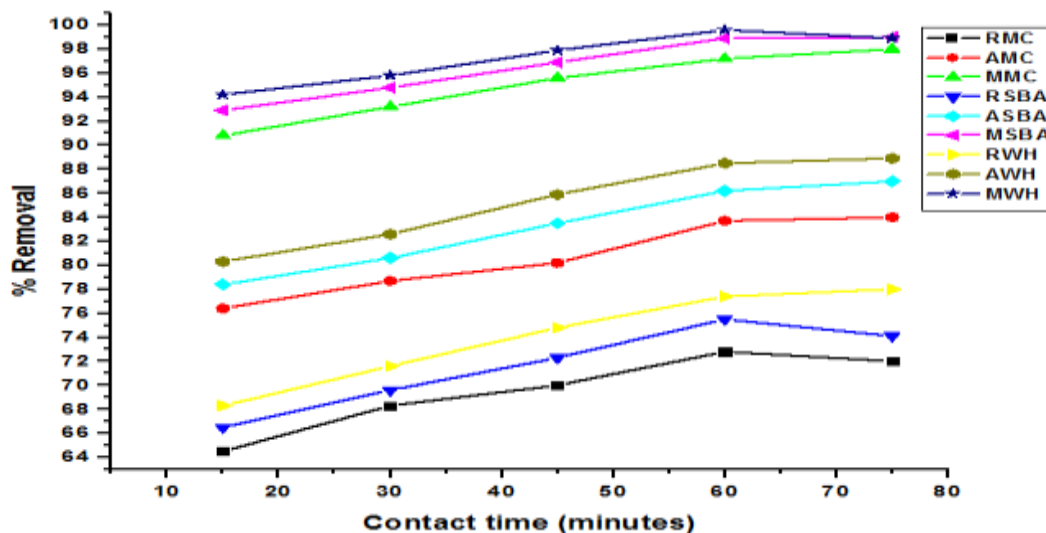


Figure 15. Effect of contact time for the removal of C.I. Acid Red 2 over RMC, AMC, MMC, RSBA, ASBA, MSBA, RWH, AWH and MWH.

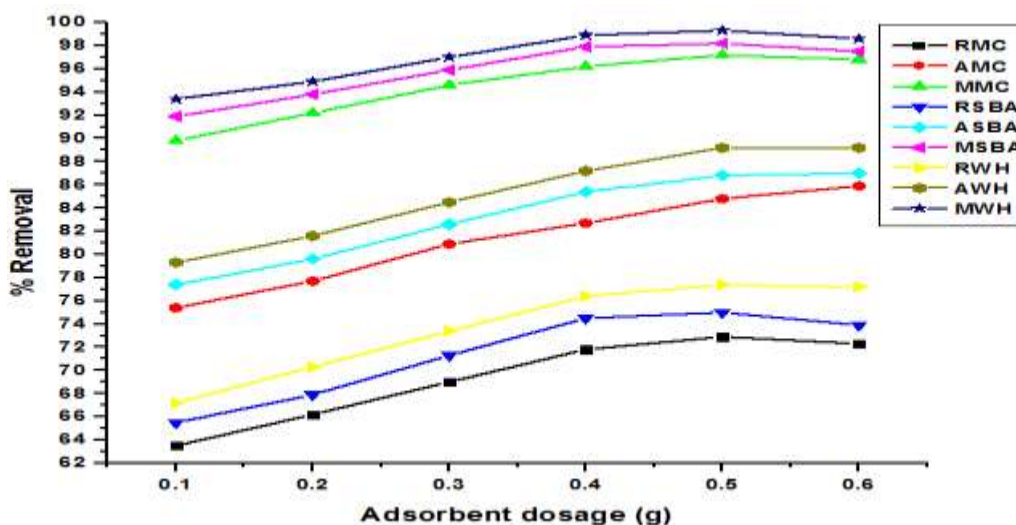


Figure 16. Effect of Adsorbent dosages for the removal of C.I. Acid Red 2 over RMC, AMC, MMC, RSBA, ASBA, MSBA, RWH, AWH and MWH.

sites and unsaturation of the sites. Greater adsorption rate was observed when the adsorbent/dye concentration ratio is greater than when the ratio is lower. Figure 16 shows the plot of adsorbent dosage versus percentage of the dye removed C.I. Acid Red 2.

From the plot, the slope is positive indicating that adsorption increases with an increase in the adsorbent dose. It can be deduced that a fixed mass of the adsorbent is needed to adsorb certain amount of the dye, which means the higher the adsorbent dose, the larger the volume of effluent can purify (Srivastava and Rupainwar, 2011). The increase in sorbent dose at

constant dye concentration and volume will lead to unsaturation of sorption sites through the sorption process.

Effect of initial dye concentration

A mass of 0.5 g of each adsorbent (RSBA, ASBA and MSBA) was contacted with 50 ml of the dye concentration 1 to 6 mg/ml at pH 2 and 5 for the adsorbents respectively, using water-bath maintained at 40°C. The agitation speed was kept constant. At

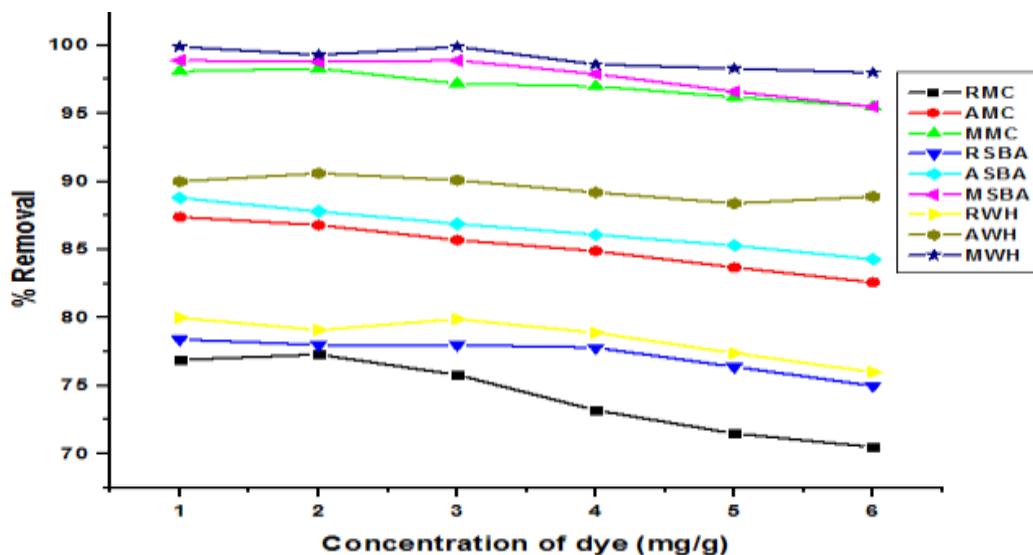


Figure 17. Effect of initial concentrations for the removal of C.I. Acid Red 2 over RMC, AMC, MMC, RSBA, ASBA, MSBA, RWH, AWH and MWH.

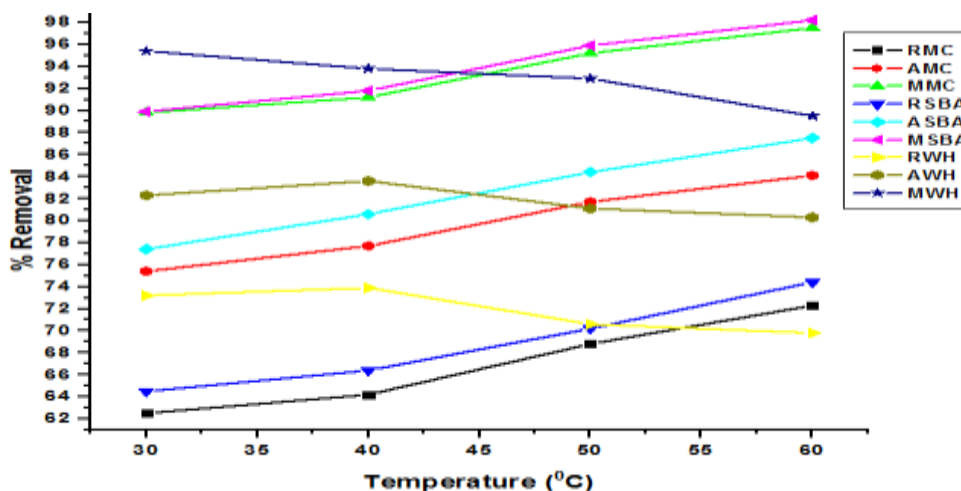


Figure 18. Effect of Temperature variation on the removal of C.I. Acid Red 2 over RMC, AMC, MMC, RSBA, ASBA, MSBA, RWH, AWH and MWH.

predetermined intervals of time, samples were analyzed for the final concentration of dyes by a UV-Vis spectrophotometer Model DR 4000 U, HACH). From the results obtained, an increase in initial dye concentration or dosage from 1-6 mg/ml leads to a decrease in the percentage of the dyes removed C.I. Acid Red 2. Figure 17 shows the plot of initial concentrations versus percentage of the dye removed C.I. Acid Red 2.

Effect of temperature

Adsorption of dye C.I. Acid Red 2 (methyl red) increased

with an increase in temperature for the adsorbents (RSBA, ASBA and MSBA) respectively. This indicates that adsorption is endothermic. The solubility of the dyes increases with an increasing temperature, thus at high temperature the dyes solution reaches an equilibrium where they can be adsorbed out by the adsorbent particle. In addition, at higher temperature the adsorbents active sites are activated thereby increasing the concentration of the dye removed. The enhancement of the adsorption might also be due to enhancement of the adsorptive interaction between the active sites and the adsorbate ion. Figure 18 shows the plot of temperature variation versus percentage of dyes (C.I. Acid Red 2)

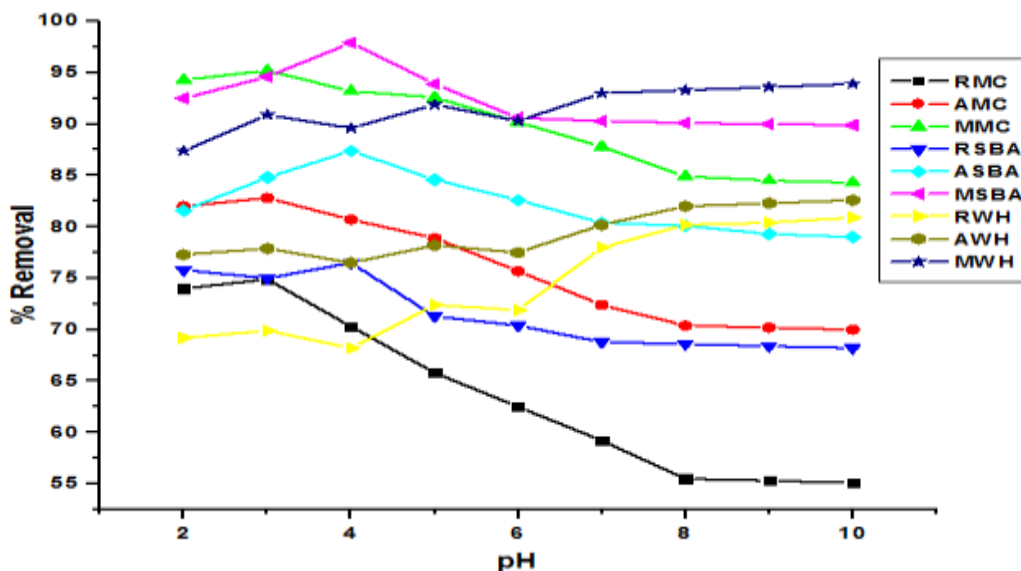


Figure 19. Effect of pH on the removal of C.I. Acid Red 2 over RMC, AMC, MMC, RSBA, ASBA, MSBA, RWH, AWH and MWH.

removed respectively.

Effect of pH

The results of the experiment done at different pH values, which were conducted to determine the optimum pH range for the dye adsorption on the surface of new biosorbents. The percentage removal of C.I. Acid Red 2 by RSBA, ASBA and MSBA was optimum at 2.5, and 4 respectively; it could be as a result of the degree of ionization of the species at the different pH. More C.I. Acid Red 2 was absorbed by RSBA, ASBA and MSBA in an acid medium. Figure 19 shows the plot of pH variation versus percentage of dyes (C.I. Acid Red 2) removed respectively.

The dyes sorption behaviour as exhibited by the three biosorbents relative to solution pH could be attributed to several reasons. The surface of all the powdered materials may contain a large number of active sites and the solute (dye ions) uptake can be related to the solute in the solution (Poinern et al., 2011).

Adsorption isotherm

Langmuir Isotherm

Adsorption isotherm is important in describing how solutes interrelate with the adsorbent and so is critical in optimizing the use of adsorbents. Correlation of isotherm data by empirical or theoretical equations is thus essential for the operation of adsorption systems and practical design (Srivastava et al., 2011). The Langmuir

equation assumes that maximum adsorption occurs when surface is covered by the adsorbate. The distribution of dyes has been described by the linear form of Langmuir equation given as:

$$(C_e/a_s) = (1/bQ_0) + (C_e/Q_0) \quad (3)$$

Where C_e is concentration of dye solution (mol L^{-1}) at equilibrium, q_e is amount of dye adsorbed per unit weight of adsorbent (mol g^{-1}), b is related to the energy of adsorption (l mol^{-1}). Figure 20 shows the Langmuir isotherm for the adsorption of C.I. Acid Red 2 by RMC, AMC, MMC, RSBA, ASBA, MSBA, RWH, AWH and MWH respectively.

The adsorption was found linear over the entire concentration range studied with good regression coefficient ($R^2 = 0.9481$ and 0.8524) for RSBA, ASBA and MSBA respectively on C.I. Acid Red 2. The result shows that the correlations fit in well into the Langmuir isotherm for C.I. Acid Red 2; this can then imply that the RSBA, ASBA and MSBA are better used to adsorb C.I. Acid Red 2 of the same concentration. It was observed to fit in correctly into Langmuir isotherms. The fact that Langmuir isotherms fits the monolayer coverage of dye very well confirms the monolayer coverage of dye on adsorbent particles and also the homogenous distribution of active sites on the material, since Langmuir equation assumes that the surface is homogenous (Saleh and Al-Absi, 2017).

Freundlich isotherm

The Freundlich model is an empirical equation based on

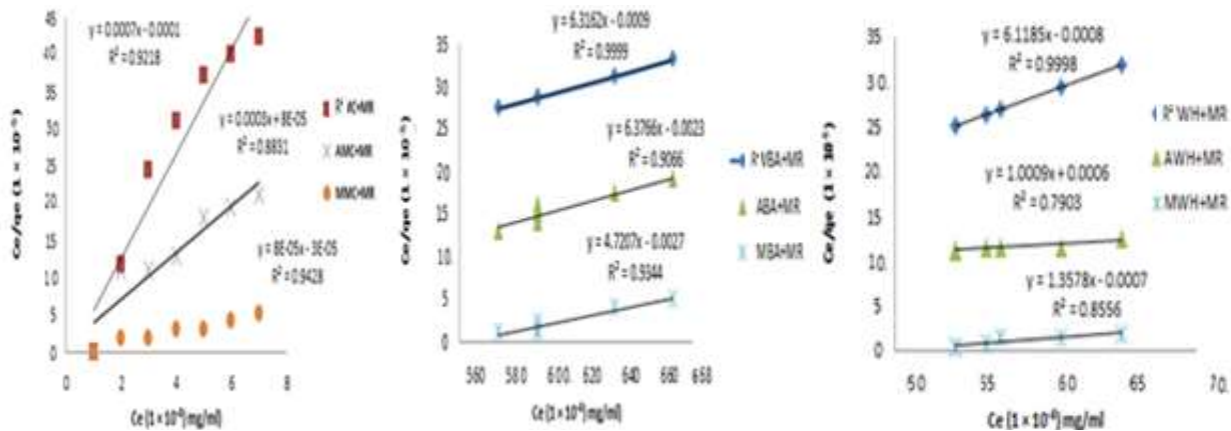


Figure 20. Langmuir isotherm for the adsorption of C.I. Acid Red 2 onto RMC, AMC, MMC, RSBA, ASBA, MSBA, RWH, AWH and MWH.

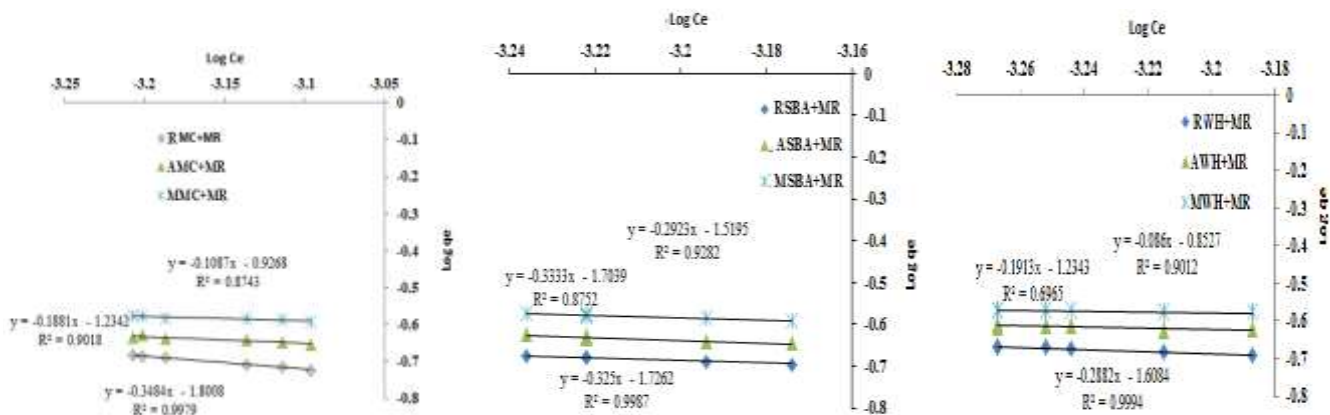


Figure 21. Freundlich isotherm for the adsorption of C.I. Acid Red 2 onto RMC, AMC, MMC, RSBA, ASBA, MSBA, RWH, AWH and MWH.

adsorption on heterogeneous surface or surface supporting sites of varied affinities. It is assumed that the stronger binding sites are occupied first and that the binding strength decreases with the increasing degree of site occupation. The Freundlich isotherms expressed (equation 4) as:

$$\log q_e = \log K_F + \frac{1}{n} \log C_e \tag{4}$$

where q_e is amount of adsorbate adsorbed per unit mass of adsorbent (mg/g); K_F is Freundlich isotherm constant (mg/g) $(L/mg)^{1/n}$, which indicate the relative adsorption capacity of the adsorbent related to the bonding energy; C_e is equilibrium concentration of the adsorbate (mg/L) and n_F is the heterogeneity factor representing the deviation from linearity of adsorption and is also known as Freundlich coefficient. If the plot of $(\log q_e)$ against $(\log C_e)$ gave straight line, it indicates that the Freundlich isotherm fit the adsorption data. Other constants can be

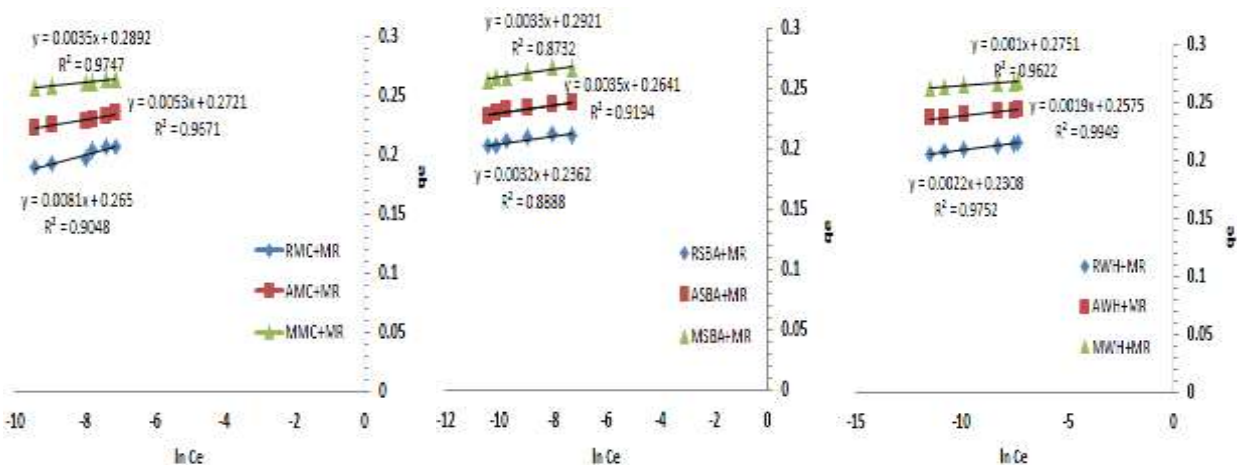
calculated from the slope ($1/n$) and intercept ($\log K_F$) of the linear plot of experimental data. The slope of $1/n$ ranging between 0 and 1 is a measure of adsorption intensity, becoming more heterogeneous as its value gets closer to zero. Figure 21 shows the Freundlich isotherm for the adsorption of C.I. Acid Red 2 by RMC, AMC, MMC, RSBA, ASBA, MSBA, RWH, AWH and MWH respectively. Table 5 shows the Langmuir and Freundlich adsorption parameter for C. I. Acid Red Dye 2.

Temkin Isotherm

This model was evaluated by using Equation 5 and plotting of (q_e) versus $(\ln C_e)$ to obtain a straight line as shown in the figure (Figure 22) with a slope (B) and intercept (B ln A), Where A is Temkin constant used to examine the interaction between RMC, AMC, MMC, RSBA, ASBA, MSBA, RWH, AWH and MWH and C.I.

Table 5. Langmuir and Freundlich adsorption parameter for C. I. Acid Red Dye.

Experimental condition	Langmuir				Freundlich			Temkin		
	q_m (mg/g)	b (L/mol)	R_L	R^2	K_F	n	R^2	A	B	R^2
RMC+MR	28.05	210.3	0.048	0.92	6.05	-2.87	0.99	162.16	0.0081	0.90
AMC+MR	333.33	63.66	0.138	0.88	3.42	-5.32	0.90	198.54	0.0053	0.96
MMC+MR	1250	2.66	11.14	0.94	2.53	-9.25	0.87	7.68	0.0035	0.97
RSBA+MR	1.58	42.25	8.62	0.99	5.64	-3.07	0.99	1.14	0.0032	0.88
ASBA+MR	1.86	57.14	6.140	0.90	5.47	-3.00	0.87	5.85	0.0035	0.91
MSBA+MR	2.12	54.38	6.756	0.93	4.57	-3.42	0.92	2.77	0.0033	0.87
RWH+MR	6.33	92.30	3.984	0.99	5.00	-3.47	0.99	3.646	0.0022	0.97
AWH+MR	7.99	94.91	3.891	0.79	3.42	-0.81	0.69	7.243	0.0019	0.99
MWH+MR	11.36	60.78	6.024	0.85	2.34	-11.63	0.90	2.981	0.0010	0.96

**Figure 22.** Temkin isotherm for the adsorption of C.I. Acid Red 2 onto RMC, AMC, MMC, RSBA, ASBA, MSBA, RWH, AWH and MWH.

based on the value of the correlation coefficient. The highest correlation coefficient value indicates the best-fit isotherm model for adsorption of C.I. Acid Red 2 (Methyl Red) dye. The adsorption parameters; q_m , K_L , n , K_f , A and B of adsorption isotherms, under the optimum experimental conditions, were also calculated and tabulated in Table 5.

$$q_e = B \ln A + B \ln C_e \quad (5)$$

Depending on this conclusion, we can say that the adsorption of C.I. Acid Red 2 dye onto RMC, AMC, MMC, RSBA, ASBA, MSBA, RWH, AWH and MWH is a heterogeneous adsorption. This means that the interaction between RMC, AMC, MMC, RSBA, ASBA, MSBA, RWH, AWH and MWH and C.I. Acid Red 2 (Methyl Red) molecules (Yargic et al., 2015). The regression relationships of the Langmuir, Freundlich and Temkin adsorption isotherms are shown in Table 6.

Adsorption kinetics

To study the mechanism and the rate by which the adsorption of C.I. Acid Red 2 (Methyl Red) onto RMC, AMC, MMC, RSBA, ASBA, MSBA, RWH, AWH and MWH occurred (mass transfer, diffusion control, or chemical reaction), different kinetic models; pseudo first-order and pseudo second-order kinetic reaction were applied to adsorption data.

Pseudo first-order kinetic model

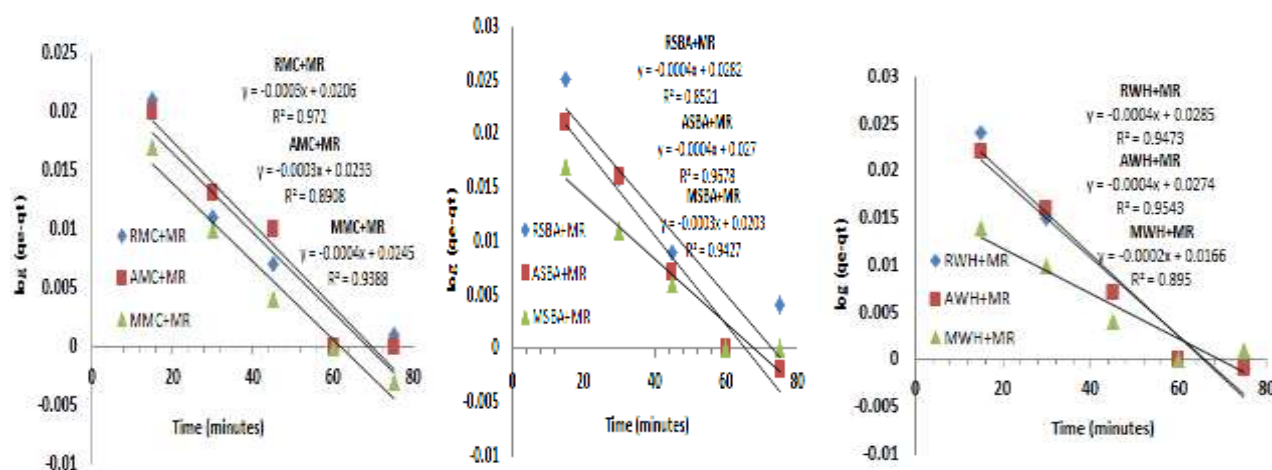
For the study of pseudo-first order kinetic model, the integral form of the Lagergren model is used for this following equation is generally used:

$$\log[q_e - q_t] = \log[q_e] - [K_1/2.303]t \quad (6)$$

Where q_e and q_t are the adsorption capacity at

Table 6. Regression relationships of the Langmuir, Freundlich and Temkin adsorption isotherms.

Experimental condition	Langmuir	Freundlich	Temkin
RMC+MR	$y=0.0007x-0.0001$ $R^2 = 0.9218$	$y = -0.3484x - 1.8008$ $R^2 = 0.9979$	$y = 0.0081x + 0.265$ $R^2 = 0.9048$
AMC+MR	$y = 0.0003x + 8E-05$ $R^2 = 0.8831$	$y = -0.1881x - 1.2342$ $R^2 = 0.9018$	$y = 0.0053x + 0.2721$ $R^2 = 0.9671$
MMC+MR	$y = 8E-05x - 3E-05$ $R^2 = 0.9428$	$y = -0.1087x - 0.9268$ $R^2 = 0.8743$	$y = 0.0035x + 0.2892$ $R^2 = 0.9747$
RSBA+MR	$y = 6.3162x - 0.0009$ $R^2 = 0.9999$	$y = -0.325x - 1.7262$ $R^2 = 0.9987$	$y = 0.0032x + 0.2362$ $R^2 = 0.8888$
ASBA+MR	$y = 6.3766x - 0.0023$ $R^2 = 0.9066$	$y = -0.3333x - 1.7039$ $R^2 = 0.8752$	$y = 0.0035x + 0.2641$ $R^2 = 0.9194$
MSBA+MR	$y = 4.7207x - 0.0027$ $R^2 = 0.9344$	$y = -0.2923x - 1.5195$ $R^2 = 0.9282$	$y = 0.0033x + 0.2921$ $R^2 = 0.8732$
RWH+MR	$y = 6.1185x - 0.0008$ $R^2 = 0.9998$	$y = -0.2882x - 1.6084$ $R^2 = 0.9994$	$y = 0.0022x + 0.2308$ $R^2 = 0.9752$
AWH+MR	$y = 1.0009x + 0.0006$ $R^2 = 0.7903$	$y = -0.1913x - 1.2343$ $R^2 = 0.6965$	$y = 0.0019x + 0.2575$ $R^2 = 0.9949$
MWH+MR	$y = 1.3578x - 0.0007$ $R^2 = 0.8556$	$y = -0.086x - 0.8527$ $R^2 = 0.9012$	$y = 0.001x + 0.2751$ $R^2 = 0.9622$

**Figure 23.** Pseudo-first order kinetic model for the adsorption of C.I. Acid Red 2 onto RMC, AMC, MMC, RSBA, ASBA, MSBA, RWH, AWH and MWH.

equilibrium and at time t , respectively (mgg^{-1}). K_1 is the pseudo first-order rate constant. Plotting of $\log(q_e - q_t)$ versus t should give a linear plot, if the adsorption process obeyed pseudo first-order kinetic model (Figure 23). The rate constants (k_1) and q_e can be calculated from the slope and intercept of the linear plot, respectively. Table 7 shows the calculated kinetic parameters of the applied pseudo first-order kinetic model.

Pseudo second-order kinetic model

The rate of adsorption is one of the most important

fundamental attributes of the adsorbent materials. To investigate pseudo second-order kinetic model, the following linear equation (7) is used:

$$\frac{t}{q_t} = \frac{1}{K_1 q_e^2} + \frac{1}{q_e} t \quad (7)$$

Where q_e , q_t , and t , were already explained above, k_2 is the rate constants of pseudo second-order kinetic adsorption. On the basis of the adsorption parameters q_e (mg/g) and K_2 the rate constant of the Pseudo second-order (g/mg-min) were calculated from the slope and the intercept respectively as in Table 8. The agreement

Table 7. The calculated first order kinetic parameters of C.I. Acid Red 2 adsorption onto RMC, AMC, MMC, RSBA, ASBA, MSBA, RWH, AWH and MWH.

Experimental materials	Pseudo-first-order kinetic model		
	q_e (mg/g)	K_1	R^2
RMC+MR	1.021	6×10^{-4}	0.97
AMC+MR	1.024	6×10^{-4}	0.89
MMC+MR	1.025	9×10^{-4}	0.93
RSBA+MR	1.028	9×10^{-4}	0.85
ASBA+MR	1.027	9.2×10^{-4}	0.96
MSBA+MR	1.021	6×10^{-4}	0.94
RWH+MR	1.028	9.2×10^{-4}	0.94
AWH+MR	1.027	9×10^{-4}	0.95
MWH+MR	1.016	4×10^{-4}	0.89

Table 8. Second-order kinetic parameters of C.I. Acid Red 2 adsorption onto RMC, AMC, MMC, RSBA, ASBA, MSBA, RWH, AWH and MWH.

Experimental materials	Pseudo- second-order kinetic model		
	q_e (mg/g)	K_2	R^2
RMC+MR	0.2012	1.9×10^{-5}	0.99
AMC+MR	0.2324	1.6×10^{-5}	0.99
MMC+MR	0.2699	1.8×10^{-5}	0.99
RSBA+MR	0.2082	1.6×10^{-5}	0.99
ASBA+MR	0.2425	1.3×10^{-5}	0.99
MSBA+MR	0.2721	2.1×10^{-5}	0.99
RWH+MR	0.2181	1.3×10^{-5}	0.99
AWH+MR	0.2476	1.4×10^{-5}	0.99
MWH+MR	0.2711	2.8×10^{-5}	0.99

between the calculated value of the q_e and the observed value of the coefficient of correlation from all the data obtained at different concentration of the dye indicates that the adsorption kinetics between adsorbent and adsorbate follow the pseudo second-order. As it is noticeable from Figure 24 and Table 8, we revealed that pseudo second-order kinetic model can best elucidate the adsorption process because it possessed a higher 0.99 R^2 value (Zare et al., 2015).

Conclusion

The result revealed the potential of RMC, AMC, MMC, RSBA, ASBA, MSBA, RWH, AWH and MWH an agricultural waste material to be an effective bio-adsorbent for removal C. I. Acid Red 2 from aqueous solution. The adsorptive removal of the C. I. Acid Red 2 onto RMC, AMC, MMC, RSBA, ASBA, MSBA, RWH, AWH and MWH can be well described by Freundlich adsorption isotherm (R^2 obtained for Freundlich model fitted more than Langmuir and Temkin model). The

adsorption capacity was found to be maximum at pH 4.4 and at adsorbent mass of 0.5 g/50 ml dye concentration within 60 min of physical adsorption. The kinetic characterization of the adsorption process on the various surfaces was well described by the pseudo second-order model. The major advantage of using bio-adsorbents for removing dyes is due to their highly selective nature of adsorption. Preliminary results indicate that RMC, AMC, MMC, RSBA, ASBA, MSBA, RWH, AWH and MWH are good bio-adsorbent for removing C. I. Acid Red 2 dye from textile wastewater.

CONFLICT OF INTERESTS

The authors have not declared any conflict of interests.

ACKNOWLEDGEMENTS

The authors appreciate The Head, Department of Chemistry and Director, Dayalbagh Educational Institute

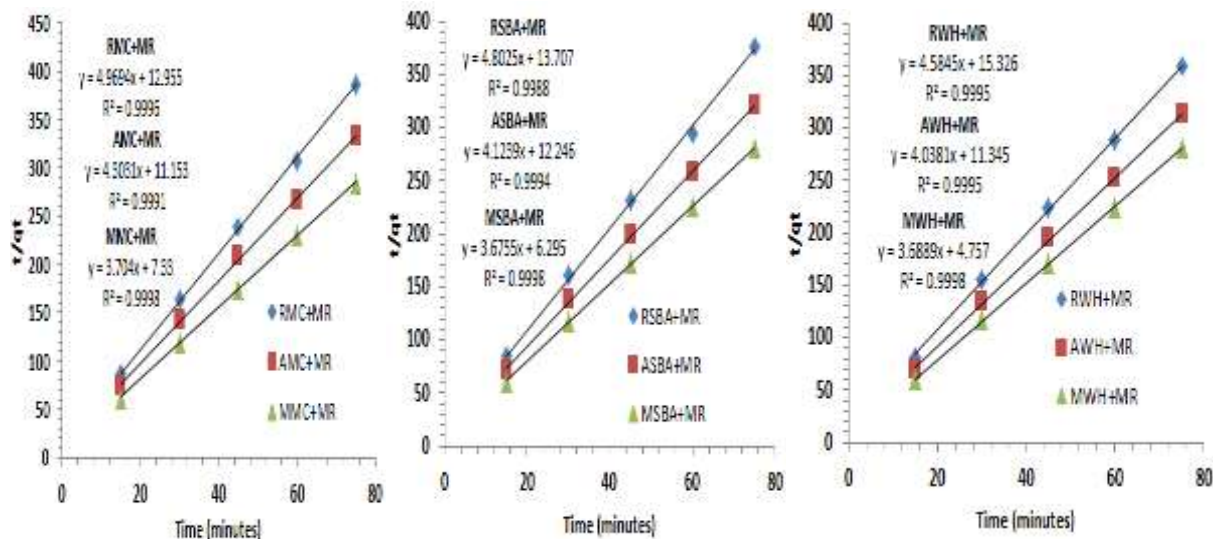


Figure 24. Pseudo-second order kinetic model for the adsorption of C.I. Acid Red 2 onto RMC, AMC, MMC, RSBA, ASBA, MSBA, RWH, AWH and MWH.

(Deemed University), Dayalbagh, Agra, India for providing required facilities to carry out this research work. The financial support from the University (DEI) under research division sustainability grant [A.R. No. 81/ Plan/Capital assets/2018/2019] is gratefully acknowledged.

REFERENCES

- Ahmad MA, Ahmad N, Bello SO (2015). Modified durian seed as adsorbent for the removal of methyl red dye from aqueous solutions. *Applied Water Science* 5:407-423.
- Alaguprathana M, Poonkothai M (2017). Decolourisation of the textile dye methyl red from aqueous solution using sugarcane bagasse pith. *Asian Journal of Advances in Agricultural Research* 3(3):1-9.
- Ardejani FD, Badii K, Limaee NY, Mahmoodi NM, Arami M, Shafaei SZ, Mirhabibi AR (2007). Numerical modeling and laboratory studies on the removal of direct red 23 and direct red 80 dyes from textile effluents using orange peel, a low cost adsorbent. *Dyes and Pigment*, 73(2):178-185.
- Azhar SS, Liew AG, Suhardy D, Hafiz KF, Hatim MDI (2005). Dye removal from aqueous solution by using adsorption on treated sugarcane bagasse. *American Journal of Applied Sciences* 2(9):1499-1503.
- Chung KT, Fulk GE, Andrews AW (1981). Mutagenicity testing of some commonly used dyes. *Applied and Environmental Microbiology* 42(4):641-648.
- Dadfarinaa S, Haji ShabaniAM, Moradi SE, Emami S (2015). Methyl red removal from water by iron based metal-organic frameworks loaded onto iron oxide nanoparticle adsorbent. *Applied Surface Science* 330:85-93.
- Dim PE (2013). Adsorption of methyl red and methyl orange using different tree bark powder. *Academic Research International* 4(1):330-338.
- Food and Agricultural Organization (FAO) (1994). *Production Year Book*. (Food and Agricultural Organization of United Nations, Rome).
- Garg VK, Amita M, Kumar R (2004). Basic dye (methylene blue) removal from simulated waste water by adsorption using Indian rose-wood saw dust: A timber industry waste. *Dyes and Pigments*, 63(3):243-250.
- Ghaedi M, Shokrollahi A, Tavallali H, Shojaiipoor F, Keshavarz B, Hossainian H, Soyak, M, Purkait MK (2011). Activated carbon and multiwalled carbon nanotubes as efficient adsorbents for removal of arsenazo (III) and methyl red from waste water. *Toxicological and Environmental Chemistry* 93(3):438-449.
- Ghaedi M, Kokhdan SN (2012). Oxidized multiwalled carbon nanotubes for the removal of methyl red (MR): kinetics and equilibrium study. *Desalination and Water Treatment* 49(1-3):317-325.
- Hameed BH (2009). Spent tea leaves, a new nonconventional and low-cost adsorbent for removal of basic dye from aqueous solutions. *Journal of Hazardous Materials* 161(2-3):753-759;
- Hassan AA, Abdulhusein HA (2015). Methyl red dye removal from aqueous solution by adsorption on rice hulls. *Journal of Babylon University/Engineering Sciences* 23(3):627-637.
- Hill G, Waage J, Phiri G (1997). The water hyacinth problems in Tropical African, *Proceedings of the First Meeting of the International Water Hyacinth Consortium*, World Bank, 18-19.
- Ioannou Z, KarasavvidisCh, Dimirkou A, Antoniadis V (2012). Adsorption of methylene blue and methyl red dyes from aqueous solutions onto modified zeolites. *Water Science and Technology* 67(5):1129-1136.
- Inthorn D, Singhtho S, Thiravetyan P, Khan E (2004). Decolourisation of basic, direct and reactive dyes by pre-treated narrow-leaved cat tail (*Typhaaugustifolia* Linn). *Bioresources Technology* 94(3):299-306.
- Jadhav DN, Vanjara AK (2004). Removal of phenol from wastewater using sawdust, polymerized sawdust and sawdust carbon. *Indian Journal of Chemical Technology* 1:194-201.
- Jadhav SU, Kalme SD, Govindwar SP (2008). Biodegradation of methyl red by galactomycesgeotrichum MTCC 1360. *International Biodeterioration and Biodegradation* 62(2):135-142.
- Janos P, Buchtova H, Ryznarova M (2003). Sorption of dyes from aqueous solutions onto fly ash. *Water Research* 37(20):4938-4944.
- Jeremias SM, Nivan BC, Luis EA (2006). Kinetics and calorimetric study of adsorption of dyes on mesoporous activated carbon prepared from coconut coir dust. *Journal of Colloid and Interface Science* 298(2):515-522.
- Klockeman DM, Toledo R, Sims KA (1997). Isolation and characterization of defatted canola meal protein, *Journal of Agricultural and Food Chemistry* 45(10):3867-3870.
- Lorenc-Grabowska E, Gryglewicz G (2007). Adsorption characteristics of congo red on coal based mesoporous activated carbon. *Dyes and Pigments* 74(1):34-40.
- Ozacar M, Sengil IA (2004). Application of kinetics models to the sorption of disperse dyes onto alunite. *Colloids and Surfaces A:*

- Physicochemical and Engineering Aspects 242(1-3):105-108.
- Poinern GEJ, Senanayake G, Shah N, Thi-Le XN, Parkinson GM (2011). Adsorption of the aurocyanide, $Au(CN)_2^-$ complex on granular activated carbons derived from macadamia nut shells-a preliminary study. *Mineral Engineering* 24(15):1694-1702.
- Prasetyko D, Ramli Z, Endud S, Hamdan H, Sulikowski B (2006). Conversion of rice husk ash to zeolite beta. *Waste Management* 26(10):1173-1179.
- Rosemal M, Haris HM, Sathasivam K (2010). Methyl red removal from water by iron based metal-organic frameworks loaded onto iron oxide nanoparticle adsorbent. *Archives of Applied Science Research* 2(5):209-216.
- Saleh TA, Al-Absi AA (2017). Kinetics, isotherms and thermodynamic evaluation of amine functionalized magnetic carbon for methyl red removal from aqueous solutions. *Journal of Molecular Liquids* 248:577-585
- Sandeep KB (2010). Adsorption Characteristics of Congo Red dye onto PAC and GAC based on S/N ratio: A Taguchi Approach, National Institute of Technology, Rourkela, India.
- Santhi T, Manonmani S, Smitha T (2010). Removal of methyl red from aqueous solution by activated carbon prepared from the *Annonasquamosa* seed by adsorption. *Chemical Engineering Research Bulletin* 14(1):11-18.
- Saxena R, Sharma S (2016). Adsorption and kinetic studies on the removal of methyl red from aqueous solutions using low-cost adsorbent: guar gum powder. *International Journal of Scientific and Engineering Research* 7(3):675-683.
- So K, Wong P, Chang K (1990). Decolorization and biodegradation of methyl red by *Acetobacterliquefaciens*. *Toxicity Assessment* 5(3):221-235.
- Srivastava R, Rupainwar DC (2011). A comparative evaluation for adsorption of dye on neemtree bark powder and mango tree bark powder. *Indian Journal of Chemical Technology* 18:67-75.
- Tanzim K, Abedin MZ (2015). A novel bioadsorbent for the removal of methyl red from aqueous solutions. *IOSR Journal of Environmental Science, Toxicology and Food Technology* 9(12):87-91.
- Tarawou T, Michael Horsfall J, Vicente JL (2007). Adsorption of methyl red by water-hyacinth (*Eichorniacrassipes*) biomass. *Chemistry and Biodiversity* 4(9):2236-2245.
- Tsai WT, Chang YM, Lai CW, Lo CC (2005). Adsorption of basic dyes in aqueous solution by clay adsorbent from regenerated bleaching earth. *Applied Clay Science* 29(2):149-154.
- Umesh K, Kaur MP, Garg VK, Sud D (2008). Removal of Nickel (II) from aqueous solution by adsorption on agricultural waste biomass using response surface methodological approach. *Bioresource Technology* 99(5):1325-1331.
- Vijayaraghavan K, Won SW, Yun YS (2009). Treatment of complex Remazol dye effluent using sawdust-and coal-based activated carbons. *Journal of Hazardous Materials* 167(1-3):790-796.
- Vijaya PP, Sandhya S (2003). Decolorization and complete degradation of methyl red by a mixed culture. *Environmentalist* 23:145-149.
- Wong P, Yuen P (1998). Decolourization and biodegradation of N,N'-dimethyl-p-phenylenediamine by *Klebsiellapneumoniae* RS-13 and *Acetobacterliquefaciens* S-1. *Journal of Applied Microbiology* 85(1):79-87
- Yargic AS, Yarbay Sahin RZ, Ozay N, Onal E (2015). Assessment of toxic copper (II) biosorption from aqueous solution by chemically-treated tomato waste. *Journal of Cleaner Production* 88:152-159,
- Yet ZR, Rahim MZA (2014). Removal of methyl red from aqueous solution by adsorption on treated banana pseudostem fibers using response surface method (rsm). *The Malaysian Journal of Analytical Sciences* 18(3):592-603,
- Yuzhu FT, Viraraghavan K (2002). Removal of congo red from an aqueous solution by fungus *Aspergillusniger*. *Advances in Environmental Research* 7(1):239-247.
- Zare K, Gupta VK, Moradi O, Makhlof ASH, Sillanpa M, Sadegh BH, Ghoshekandi RS, Pal A, Wang ZJ, Tyagi I, Kazemi M (2015). A comparative study on the basis of adsorption capacity between CNTs and activated carbon as adsorbents for removal of noxious synthetic dyes: a review. *Journal of Nanostructure in Chemistry* 5:227-236.
- Zollinger H (1987). *Colour Chemistry-Synthesis, Properties and application of organic dyes and pigments*, New York: VCH Publishers, NII Article ID (NAID) 10011739210.